Journal of Nuclear Materials 381 (2008) 62–67

Contents lists available at ScienceDirect

Journal of Nuclear Materials

journal homepage: www.elsevier.com/locate/jnucmat

Dimensional and material property changes to irradiated Gilsocarbon graphite irradiated between 650 and 750 °C

Barry J. Marsden [a,*], Graham N. Hall [a], Onne Wouters [b], J.A. Vreeling [b], J. van der Laan [b]

[a] Nuclear Graphite Research Group, School of Mechanical, Aerospace and Civil Engineering, The University of Manchester, Manchester, United Kingdom
[b] Nuclear Research and Consultancy Group, P.O. Box 25, 1755 ZG, Petten, The Netherlands

A B S T R A C T

Samples of Gilsocarbon graphite have been recently irradiated in the High Flux Reactor at Petten. They were irradiated in an inert atmosphere to a fast neutron dose of between 3 and 10 dpa, at temperatures of between 650 and 750 °C, this irradiation dose equates to approximately dimensional change 'turn-around'. The present understanding of the irradiation induced microstructural changes considered to lead to the irradiation induced dimensional and material property changes are discussed and correlations between the various property changes noted. However, at present there are few microstructural studies to confirm or refute these theories. A methodology proposed to convert graphite CTE measurement, for all types graphite, from one temperature range to another is shown to be applicable to both unirradiated and irradiated Gilsocarbon graphite. In addition an important relationship for the thermal conductivity temperature dependence of irradiated Gilsocarbon graphite is shown to be reasonable.

1. Introduction

For nuclear applications Gilsocarbon graphite was manufactured between the 1960s through to the 1980s. Its excellent nuclear properties arise from the microstructure of the Gilsonite coke which was obtained as a bi-product from the processing of Gilsonite pitch mined in Utah [1]. The microstructure of the Gilsonite coke particles is illustrated in the HRTEM, SEM and optical images given in Figs. 1(a)–(d). At the nano-scale, within the graphite crystallites, many Mrozowski cracks [2] a few nanometres in width by several micrometres long provide accommodation that can take up crystal 'c' axis thermal expansion and fast neutron induced 'c' axis crystal expansion [3], see Fig. 1(a). At a larger scale, Fig. 1(b), the microstructure is shown to consist of many graphite platelets, shown in the SEM image Fig. 1(b), and at a slightly larger scale the porosity caused by gas evolution can clearly be seen in the SEM image, Fig. 1(c). The tiny crack-like features (Mrozowski cracks) are reflected at a larger scale as clearly seen under the optical microscope (see Fig. 1(d)). Thus accommodation for the large irradiation induced crystal expansion is provided from the nanometre scale through to micrometre scale. The existence and importance of these crack-like features in nuclear graphite is not unique to Gilsocarbon graphite, however it is the arrangement of these flawed crystallite structures into spherical 'filler' particles about 0.5mm diameter that gives Gilsocarbon graphite its semi-isotropic material properties up to significantly high irradiation dose, thus ameliorating the potential for high irradiation induced stresses in reactor graphite components. Gilsocarbon graphite was used as a moderator in all of the UK AGRs, the THTR in Germany and as fuel supports in some French Magnox reactors. For this reason there is an extensive empirical irradiated Gilsocarbon database particularly for irradiation temperatures below 650 °C. However, there have been no systematic studies of the irradiation induced microstructural change and how this relates to dimensional and material property change. For this reason Gilsocarbon graphite samples have recently been irradiated at HFR Petten. This paper details the irradiation experiments, presents the initial irradiation data and makes comparisons to previous Gilsocarbon irradiation data (see Fig. 2).

2. Irradiation programme

The irradiation was carried out in an inert helium atmosphere in the High Flux Reactor (HFR) at Petten. Fifteen samples, nominally 8 mm diameter by 12 mm or 6 mm, long were irradiated to a fast neutron dose of between 3.4 and 9.15 dpa[1]. Ten of the specimens were irradiated at 750 °C and five were irradiated at a slightly lower temperature in the range 650–700 °C.

The following material properties were measured both prior to and after irradiation: individual sample dimensions, thermal conductivity (via thermal diffusivity), coefficient of thermal expansion (CTE), dynamic Young's modulus, mass and volume (hence

* Corresponding author. Tel.: +44 161 275 4399.
E-mail address: barry.marsden@manchester.ac.uk (B.J. Marsden).

[1] In graphite, by definition, 1 n cm^{-2} EDND = 1.313 × 10^{-21} displacement per atom (dpa).

0022-3115/$ - see front matter © 2008 Elsevier B.V. All rights reserved.
doi:10.1016/j.jnucmat.2008.07.018

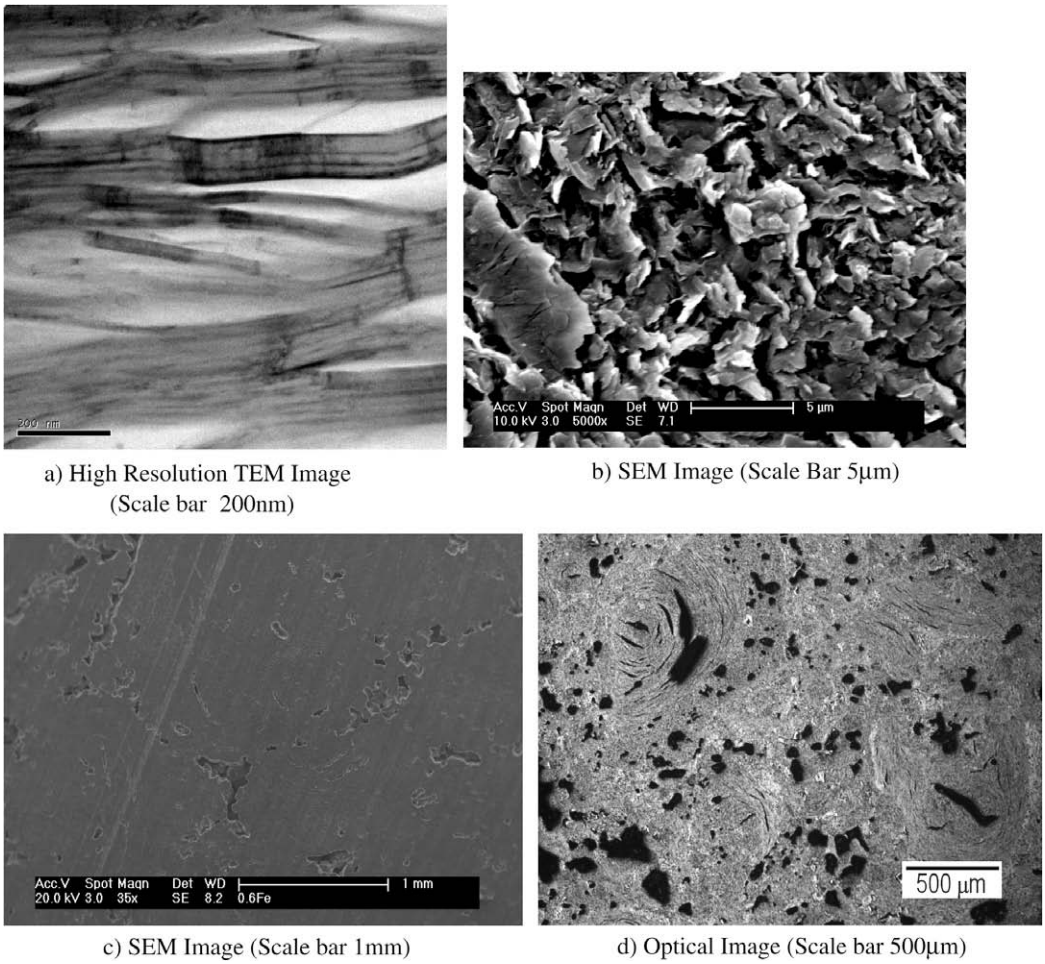

a) High Resolution TEM Image (Scale bar 200nm)

b) SEM Image (Scale Bar 5µm)

c) SEM Image (Scale bar 1mm)

d) Optical Image (Scale bar 500µm)

Fig. 1. HRTEM, SEM and optical images showing the unirradiated Gilsocarbon graphite microstructure: (a) high resolution TEM image (scale bar 200 nm), (b) SEM image (scale bar 5 μm), (c) SEM image (scale bar 1 mm) and (d) optical image (scale bar 500 μm).

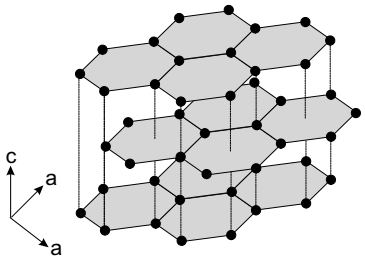

Fig. 2. Graphite crystal structure.

density). In the post irradiation examination all these properties are measured on all specimens, with the exception of the 12 mm specimens, of which no thermal diffusivity could be measured. Before irradiation, reference thermal diffusivity and CTE measurements were performed on a selection of specimens. For every two neighbouring specimens machined out of the original block of material one is measured and the other is assumed to have the same thermal properties. The other properties prior to irradiation are determined for all specimens.

Sample dimensions were measured before and after the irradiation using Mahr inductive probes (Mahr, type P 2104 MB) with a measurement range of 4 mm and an accuracy of 0.1 μm. The measurement is a comparison of the dimensions of a well-known calibre and the specimen. The volume of each specimen is calculated based on the measured dimensions. The mass of each specimen is determined with a Mettler AT261 scale with an accuracy of 0.01 mg. The dynamic Young's modulus was determined by measuring the velocity of sound in the sample. The velocity of sound is determined with an Agfa-Krautkramer USM 25, using a nominal frequency of 5 MHz. The set-up is calibrated using a steel sample with a known velocity of sound.

The coefficient of thermal expansion was measured using a Netzsch dilatometer DIL402C over the temperature range 25–750 °C. Finally, thermal diffusivity was measured using the laser flash method on a Netzsch LFA457 MicroFlash. Thermal conductivity values were derived from the thermal diffusivity data by multiplication with density and specific heat (ASTM C781).

3. Properties of unirradiated and irradiated nuclear graphite

To obtain a reasonably isotropic product the Gilsocarbon graphite irradiated in this programme was manufactured by moulding, i.e. by pressing from one, or both ends to form the final billet shape before baking and graphitising. This process produces a distinct 'grain' direction. Against Grain 'AG' is parallel to the pressing direction and With Grain 'WG' is perpendicular to the pressing direction. It should be noted that in extruded grades of nuclear graphite the 'WG' directions is parallel to billet extrusion direction.

The unirradiated, and irradiated, graphite properties can be related to the WG and AG directions, via the theoretical graphite

crystal properties, by the present understanding of the graphite microstructure and irradiation induced microstructural changes.

4. Graphite crystal/crystallites

- The graphite crystal has strong bonds in the basal plane '*a*' direction but weak bonds between basal planes '*c*' direction therefore:
  - The crystal is stiffer (modulus greater) in the '*a*' basal plane than perpendicular to the basal plane.
  - The crystal is stronger in the '*a*' basal plane than perpendicular to the basal plane.
- With irradiation the graphite crystal shrinks in the direction of the basal plane '*a*' direction and swells perpendicular to the basal planes '*c*' direction. Also the rate of shrinkage/swelling is greater in the '*c*' direction than in the '*a*' direction. However, within the 'graphite crystallite' structures there are accommodation cracks, which can take up the '*c*' growth. Therefore, if the crystal is restrained, only the '*a*' axis shrinkage will be observed until these cracks are filled.
- The coefficient of thermal expansion is much greater in the '*c*' direction than in the '*a*' direction. However, if the crystal is restrained thermal expansion can be accommodated by the 'accommodation cracks'.
- Within the crystal the main mechanism for heat transfer is lattice vibration along the basal plane. Thus thermal conductivity is much higher along the basal plane than perpendicular to the basal plane. As the temperature increases phonon–phonon scattering increases and the efficiency of conductivity along the basal planes decreases; therefore thermal conductivity also decreases. Irradiation causes defects in the graphite lattice and this also reduces thermal conductivity along the basal plane.

5. Polycrystalline graphite

When polycrystalline graphite is manufactured either by extrusion, moulding or iso-moulding there is always some degree of preferred orientation, referred to as with grain (WG) or against grain (AG).

In the WG case most of the graphite crystals are aligned along the grain direction.

In the AG case most of the crystals are aligned against the grain direction.

The virgin polycrystalline properties can therefore be understood from the crystallite properties. Virgin polycrystalline graphite, therefore:

1. Has a higher modulus in the WG direction than in the AG direction.
2. Is stronger in the WG direction than in the AG direction.
3. Has a lower CTE in the WG direction than in the AG direction.
4. Has a higher thermal conductivity in the WG direction than in the AG direction.

There is good evidence to support the above statements.

To some extent the irradiated properties also can be understood from the crystal properties. Irradiated (non-oxidised) polycrystalline graphite, therefore:

1. Shrinks faster in the WG direction than in the AG direction. (The crystal '*c*' swelling being taken up by the accommodation cracks.)
2. Turns around quicker in the AG direction than in the WG direction. (After the '*c*' axis accommodation has been filled.)
3. At low dose there is a rapid decrease in thermal conductivity mainly due to irradiation induced defects within the basal plane. At high irradiation dose there is a second decrease in thermal conductivity as the crystal structure is degraded due to the large crystallite dimensional change.
4. CTE behaviour is far from fully understood, but the initial rise is thought to be due to crack closure.
5. Modulus behaviour is not fully understood, although the initial rise is thought to be related to 'pinning', and the secondary rise appears to be related to crack closure. At even higher dose as the structure degrades due to large crystallite dimensional change the modulus starts to decrease.
6. Strength appears to be correlated with modulus.
7. Irradiation creep behaviour of nuclear graphite (not examined in this experiment) is not fully understood and appears to be a function of stress, dose and modulus.

6. Gilsocarbon irradiation results

Individual pre irradiation and post irradiation sample measurements were made on most of the samples, although in some cases only the neighbouring post irradiation properties were measured. The relevant unirradiated properties are given in Table 1. Sample orientation denoted by *x*, *y* and *z* is related to the block of Gilsocarbon supplied. Although these directions are orthogonal to the manufacturing grain unfortunately they cannot be related to the moulding direction (pressing). However, it can be seen from the measurements shown in the figures that both the unirradiated and irradiated properties of this particular grade of Gilsocarbon are near isotropic.

6.1. Dimensional change

Fig. 3 shows the dimensional change behaviour; the curves added for guidance are based on a statistical analysis by Eason et al. [4] for various grades of Gilsocarbon graphite irradiated at temperatures between ~300 and ~650 °C. Although the use of this empirical fit to this higher temperature data is not ideal, the fits indicate that the samples reported here are approaching dimensional change 'turn-around'. Although the present data shows some degree on anisotropy it is less that than would be defined by the Eason lower temperature fit, In the dimensional change behaviour of all grades of Gilsocarbon graphite, at this irradiation temperature, there is a point of inflection around 25×10^{20} n cm^{-2} Equivalent Dido Nickel Dose (EDND). This point of inflection is important as it usually co-insides with the maximum component early life stress [5]. The initial expansion in dimensional change at very low irradiation dose has been attributed to the annealing

Table 1
Unirradiated Gilsocarbon sample properties

Property	Mean	Standard deviation	*N*
Density (g/cm^3)	1.79	0.01	15
E_x (GPa)	10.14	0.20	5
E_y (GPa)	10.02	0.16	4
E_z (GPa)	10.19	0.10	6
α (20–120 °C)$_x$ (K^{-1})	4.52	0.12	5
α (20–120 °C)$_y$ (K^{-1})	4.58	0.31	4
α (20–120 °C)$_z$ (K^{-1})	4.47	0.20	6
K (25)$_x$ (W/m/K)	132.77	0.45	2
K(25)$_y$ (W/m/K)	129.78	1.00	2
K(25)$_z$ (W/m/K)	131.46	3.38	2

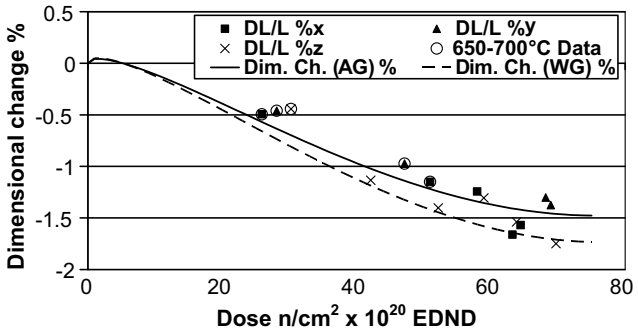

Fig. 3. Linear dimensional change with fast neutron dose.

out of internal stresses, although there is no validation to confirm this speculation. It is, therefore, unfortunate there is no low dose data to define the early part of the curve and for use in microstructural studies.

6.2. Thermal expansion coefficient

The measurements of the coefficient of thermal expansion (CTE) are given in Fig. 4. Measurements have been made over three temperature ranges 30–120 °C, 30–200 °C, 30–750 °C. Recent work reported by Tsang et al. [6] proposed a linear relationship between the mean CTE in the range 20–120 °C and the CTE over some other range 20–T °C using the following relationship:

$$\alpha_{(20-T)} = \bar{\alpha}_{(20-120\,^\circ\mathrm{C})} + \bar{B}(T),$$

$$\bar{B}(T) = -0.225966 + 0.00201886T + 3.89449 \times 10^{-8}T^2 - 8.38187 \times 10^{-10}T^3 + 3.153526 \times 10^{-13}T^4.$$

Note the difference between the value of mean CTE over the ranges 20–120 °C and 30–120 °C will be insignificant.

Using this formula $\bar{B}(T)$ is calculated as $0.17 \times 10^{-6}\,\mathrm{K}^{-1}$ and $1.06 \times 10^{-6}\,\mathrm{K}^{-1}$ for conversion of the mean CTE over the range 20–120 °C to the range 20–200 °C and 20–750 °C, respectively, see Table 2. From the present irradiation measurement the values of $\bar{B}(T)$ given in Table 2 were calculated. Both the experimental irradiated and non-irradiated factors are similar and considering these values would be additive to CTE values in the range $2–5 \times 10^{-6}\,\mathrm{K}^{-1}$ they compare well with the values predicted by Tsang et al. [6] providing some confidence in the use of this methodology for irradiated non-oxidised graphite.

Table 2
Experimental values of $\bar{B}(T)$ ($\times 10^{-6}\,\mathrm{K}^{-1}$) to those due to Tsang et al. [6]

	Irradiated factor $\bar{B}(T)$ 30–200 °C	Irradiated factor $\bar{B}(T)$ 30–750 °C	Non-irradiated factor $\bar{B}(T)$ 30–200 °C	Non-irradiated factor $\bar{B}(T)$ 30–750 °C
Exp. mean	0.10	1.17	0.11	1.13
Exp. σ	0.09	0.19	0.19	0.19
Tsang et al. [6]	0.17	1.06	0.17	1.06

The present irradiated CTE data predicts the expected rise in CTE attributed to closure of Mrozowski cracks. The fall in CTE is also typical of the irradiation of medium grained nuclear graphite. However the mechanism that causes this reduction in CTE with increased dose is less certain and is not typical of some coarser grained graphites, such as Pile Grade A (PGA) [7]. High resolution microstructural studies on irradiated graphite samples are required to determine the reasons for this behaviour.

6.3. Young's modulus

The measurements of the irradiation induced changes to Young's modulus are given in Fig. 5. As there are insufficient data to fit the complex shape that defines the change in modulus with dose a trend line has been drawn through the data by hand in order to illustrate the various aspects of modulus change. Unfortunately there are not enough low dose data to define the exact shape of the initial rise in modulus, which has been attributed to 'pinning' of dislocations in the basal plane. Although it is unclear exactly what this pinning mechanism is and the authors know of no microstructural observations that can be linked to the change. The second rise in modulus has been related to an increase due to internal stressing caused by dimensional change, although modelling work by Hall et al. [8] attributed this rise to stiffing due to Mrozowski crack closure. Further irradiation would be expected to lead to a rapid reduction in modulus due to degeneration of the microstructure due to significant irradiation induced swelling of the crystallite.

6.4. Thermal conductivity

At temperatures of interest for nuclear reactors the mechanism of thermal conduction in graphite is due thermal vibration of the crystal lattice [9]. In unirradiated graphite phonon scattering is increased with increasing temperature thus reducing the thermal conductivity. Irradiation induced lattice defects also increase phonon scattering significantly reducing thermal conductivity.

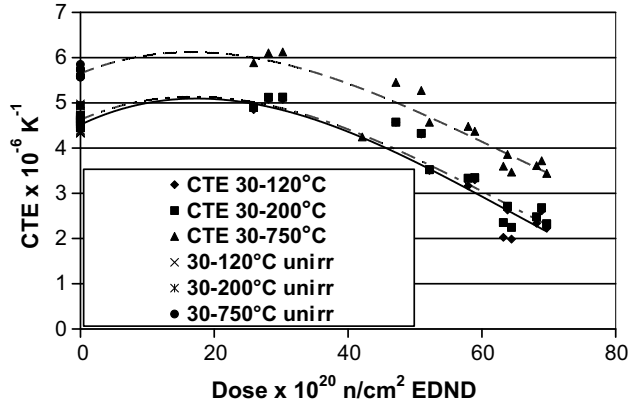

Fig. 4. Change in coefficient of thermal expansion with fast neutron dose.

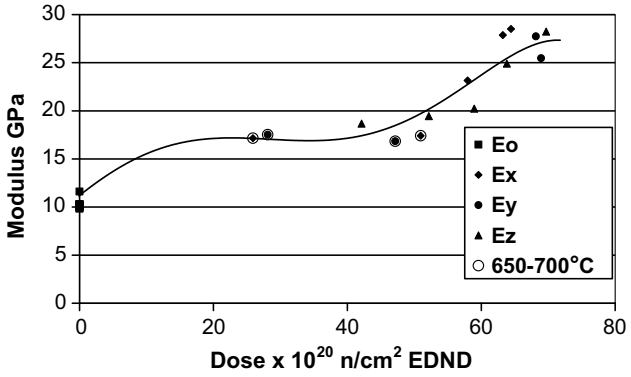

Fig. 5. Change in Young's modulus with fast neutron dose.

However, the irradiation induced decrease in thermal conductivity soon saturates with dose. At high irradiation dose there is a secondary decrease in thermal conductivity attributed to structural micro-cracking. As can be seen from Fig. 6 thermal conductivity of Gilsocarbon graphite irradiated at this temperature quickly reduces with irradiation dose. In the nuclear industry thermal conductivity is usually quoted as change in thermal resistivity (the reciprocal of thermal conductivity). Thermal resistivity results from this study are therefore presented, at various measurement temperatures, in Fig. 6. Over the measurement range there appears to be a slight increase in thermal resistivity with increased dose, which may be due to high dose structural changes as discussed above, although the main high dose reduction in thermal conductivity would be expected to co-inside with a reduction in modulus, this irradiation dose was not reached in these particular experiments. Thermal conductivity has been measured at various temperatures, the higher the temperature the higher the thermal conductivity. This is the opposite from the behaviour of unirradiated Gilsocarbon graphite as illustrated in Fig. 7. This change to the temperature dependence in irradiated graphite was noted by Kelly [10] who proposed the following formula for calculating the thermal resistivity of irradiated graphite:

$$\frac{1}{K(T)} = \frac{1}{K_o(30)}\left[\frac{K_o(30)}{K_o(T)} + f \cdot \delta(T)\right] S_k,$$

where the initial irradiation induced change in thermal resistivity is given by $f = \frac{K_o(30)}{K_i(30)} = \frac{K_o(30)}{K(30)} - 1$ and S_k is a structural term to allow for the secondary decrease of thermal conductivity at higher dose. Both of these relationships need to be obtained empirically as a function

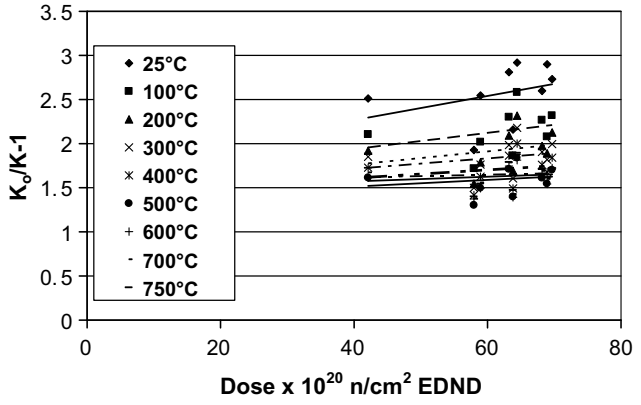

Fig. 6. Change of thermal resistivity with fast neutron dose as a function of dose and measurement temperature.

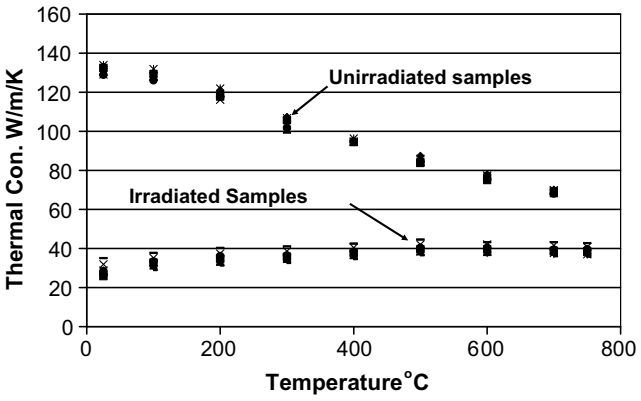

Fig. 7. Unirradiated and irradiated thermal conductivity temperature dependence of Gilsocarbon graphite.

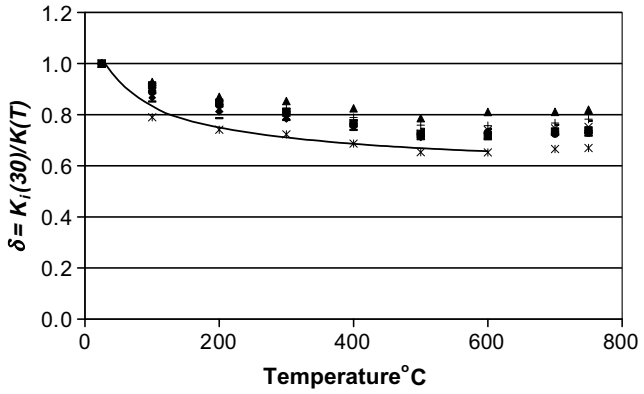

Fig. 8. Comparison of 'δ-curves' for irradiated graphite.

of both irradiation temperature and dose from Material Test Reactor (MTR) experiments. The change in unirradiated thermal resistivity $\frac{K_i(30)}{K_o(T)}$ is a function of measurement temperature only and should be obtained on the particular graphite of interest. The factor $\delta = \frac{K_i(30)}{K(T)}$ is the irradiated dependence of thermal resistivity as a function of temperature. Various forms of this 'δ-curve' have been proposed based on irradiation experiments carried out on Highly Orientated Pyrolytic Graphite (HOPG) [11,12] and assuming that as the conductivity along the basal planes is much higher than perpendicular to the plane that only conduction in the crystallographic '*a*' direction need to be considered. The latest version of the δ-curve is plotted in Fig. 8 along with δ-curves obtained from the present irradiation study. Considering the existing δ-curve was derived from HOPG data the trend and magnitude of the curves gives some confidence in the Kelly [10] method when applied to non-oxidised graphite.

6.5. Correlation between irradiation induced changes

From the irradiation data available the following features can be observed:

- There is an inflection in the dimensional change behaviour, between about 20–30 $\times$ 10^{20} n cm^{-2} EDND which denotes a change in dimensional change rate.
- This change in dimensional change rate appears to be associated with the peak in the CTE curve.
- Both the peak in CTE and change in dimensional change rate appear to be associated with the closure of the smaller Mrozowski type cracks although microstructural observation is required to validate this.
- There is a secondary increase in Young's modulus about 40–50 $\times$ 10^{20} n cm^{-2} EDND. There also appears to be indication of the start of the secondary increase in thermal resistivity, although a more rapid increase would be expected at a higher dose coinciding with a decrease in Young's modulus.

7. Conclusions

1. Data for semi-isotropic Gilsocarbon graphite irradiated approximately to the point of dimensional change 'turn-around' at temperatures between 650 and 750 °C is presented.
2. The dimensional change data follows the same trend with dose as previously irradiated Gilsocarbon graphite.
3. With increasing dose the coefficient of thermal expansion increases before falling. The factor required to convert between CTE temperature ranges appear to be the same for both unirradiated and irradiated graphite and compares well with values obtained using a recently published theory.

4. Young's modulus appears to have reached the second irradiated induced increase attributed to micro-crack closure; there is also indication of a secondary increase in thermal resistivity, although a more rapid increase in thermal resistivity would be expected at a higher dose that was reached in these experiments.
5. The thermal conductivity temperature dependence is modified by irradiation. The irradiated thermal conductivity temperature dependence obtained in this irradiation programme is similar in magnitude and trend to that previously proposed by Kelly.
6. Microstructural studies on the irradiated samples are required in order to try and establish the mechanisms involved in these dimensional changes. In addition; samples irradiated to a lower dose are required to establish the first part of the relationships.

Acknowledgments

The TEM, SEM and optical images in Fig. 1 are attributed to Dr Mark Joyce, Dr Keyun Wen and Dr Abbie Jones of the Nuclear Graphite Research Group, The University of Manchester. This work was carried out as part of the TSEC programme KNOO and as such we are grateful to the EPSRC for funding under grant EP/C549465/1.

References

[1] H.F. Kretchman, The Story of Gilsonite, American Gilsonite Company, Salt Lake City, Utah, 1957.
[2] S. Mrozowski, Mechanical strength, thermal expansion and structure of cokes and carbons, in: First Biennial Conference on Carbon, University of Buffalo, Buffalo, 1953.
[3] J.E. Brocklehurst, B.T. Kelly, The dimensional changes of highly oriented pyrolytic graphite irradiated with fast neutrons at 430 °C and 600 °C, Carbon 31 (1) (1993) 179.
[4] E.D. Eason, G. Hall, B.J. Marsden, Development of a model of dimensional change in AGR graphites irradiated in inert environments, in: Ageing Management of Graphite Reactor Cores Conference, 28–30th November, 2005.
[5] D.K.L. Tsang, B.J. Marsden, J. Nucl. Mater. 350 (3) (2006) 208.
[6] D.K.L. Tsang, B.J. Marsden, S.L. Fok, G. Hall, Carbon 43 (2005) 2902.
[7] J.E. Brocklehurst, B.T. Kelly, Carbon 31 (1) (1993) 155.
[8] G. Hall, B.J. Marsden, S.L. Fok, J. Nucl. Mater. 353 (1–2) (2006) 12.
[9] B.T. Kelly, Physics of graphite, Applied Science, London, 1981.
[10] B.T. Kelly, An improved method of estimating the thermal conductivity of irradiated graphite at any temperature, AB 7/19346, available from the UK Public Records Office, 1967.
[11] R. Taylor, Philos. Magn. 13 (121) (1966) 157.
[12] R. Taylor, B.T. Kelly, K.E. Gilchrist, J. Phys. Chem. Solids 30 (1969) 225l.